IEEE Access
Multidisciplinary ⋮ Rapid Review ⋮ Open Access Journal

Received 7 April 2024, accepted 29 April 2024, date of publication 6 May 2024, date of current version 20 May 2024.

Digital Object Identifier 10.1109/ACCESS.2024.3397165

RESEARCH ARTICLE

Bandwidth Allocation and Power Control Optimization for Multi-UAVs Enabled 6G Network

MOHAMMAD AHMED ALNAKHLI[1], (Member, IEEE), EHAB MAHMOUD MOHAMED[1], (Member, IEEE), AND MOSTAFA M. FOUDA[2,3], (Senior Member, IEEE)

[1]Department of Electrical Engineering, College of Engineering in Wadi Addwasir, Prince Sattam bin Abdulaziz University, Wadi ad-Dawasir 11991, Saudi Arabia
[2]Department of Electrical and Computer Engineering, Idaho State University, Pocatello, ID 83209, USA
[3]Center for Advanced Energy Studies (CAES), Idaho Falls, ID 83401, USA

Corresponding author: Mohammad Ahmed Alnakhli (m.alnakhli@psau.edu.sa)

This work was supported by Prince Sattam bin Abdulaziz University under Project PSAU/2024/R/1445.

ABSTRACT In this paper, we undertake an examination of the complicated challenges associated with bandwidth allocation and power control in multi- unmanned aerial vehicles (UAVs) network. The focal point of our investigation is the formulation and subsequent proposition of a novel algorithm aimed at optimizing bandwidth utilization and energy efficiency across multiple UAVs. The intricate joint optimization problem is cast as a nontrivial nonlinear programming (NLP) challenge; thus, to efficiently address it, we split it into two subproblems. In the first sub-problem, UAVs bandwidth resources are being optimized while considering that they are operating at their maximum transmit powers. In the second sub-problem and after optimizing bandwidth allocations, UAVs transmit powers are optimized based on their inter-links speed. Sequential quadratic programing (SQP) based on coloring graph representation is proposed to address the first sub-problem, while $\mathcal{M}$- matrix theory is employed to address the second one. Rigorous numerical simulations are conducted to prove the effectiveness of the proposed scheme against other benchmarks in maximizing both data rate and energy efficiency of the proposed multi-UAV network.

INDEX TERMS 6G, multi-UAVs, spectrum efficiency, energy efficiency, SQP, $\mathcal{M}$-matrix.

I. INTRODUCTION

Unmanned aerial vehicles (UAVs) are expected to play a significant role in the beyond fifth generation (B5G) and six generation (6G) wireless networks in the next decade [1]. The deployment of UAVs is ever-increasing, and the number of commercial UAV fleets can reach up to 1.6 million by 2024 [2]. UAVs can be dispatched as high-mobility aerial communication platforms to provide opportunistic line-of-sight (LoS) links and further assist terrestrial communications in 6G [3]. The integration of UAVs into 6G networks has numerous use cases, including base station (BS) offloading, swift service recovery after natural disasters, emergency response, rescue and search, information dissemination, and data collection from the internet of things (IoTs) devices, and mounting reconfigurable intelligent surface (RISs) boards [4], [5]. However, the incorporation of UAVs into 6G networks calls for a paradigm shift in the design of both cellular and UAV communication systems due to the high altitude and mobility of UAVs, the unique channel characteristics of UAV-ground links, the asymmetric quality of downlink and uplink data transmission, the stringent constraints imposed by the size, weight, power limitations of UAVs, and the intra-system and inter-system interference of the integrated networks [6]. Key challenges associated with the widespread commercial use of UAVs towards 6G include safety, traffic control, and security aspects [2]. Moreover, researchers are interested in

The associate editor coordinating the review of this manuscript and approving it for publication was Xijun Wang.

developing green UAV communication with low power consumption to prolong UAVs' lifetime [4], [7].

Multi-UAV is a promising solution for coverage area problems, especially for 6G networks. The scalability of multi-UAV systems aligns seamlessly with the expansive nature of 6G applications, making them well-suited for urban environments, remote areas, and critical infrastructure inspection. Through coordinated multi-UAVs, these UAVs contribute to optimizing coverage, resource utilization, and network reliability, thereby positioning themselves as integral components in the realization of resilient and high-performing communication networks in the era of 6G. In this context, researchers have proposed various frameworks for persistent multi-UAV coverage with global deconfliction such as UAV gateway selection given in [8].

In this paper, we will tackle the problem of optimal bandwidth and power allocations in multi-UAV enabled 6G network. In this regard, we will make use of graph theory [9] for bandwidth optimization. Besides bandwidth allocation, efficient power control in multi-UAV scenarios is essential for overall system performance, interference management, and resource utilization, considering the limited battery capacities of UAVs [7]. Thus, in this paper, $\mathcal{M}$-matrix theory will be utilized as an efficient tool for UAVs power control. Thus, the main contributions of this paper can be summarized as follows:

- A two-step algorithmic approach will be proposed to address the problem of bandwidth allocation and power control in multi-UAV networks. In the first step, bandwidth allocations are optimized while assuming UAVs are transmitting at their maximum power. In the second step, UAVs transmit powers are optimized based on their inter-link speeds result from their optimized bandwidth allocations done in the first step.
- Graph theory in the form of coloring graph will be proposed for UAVs bandwidth allocation optimization. In this regard, graph theory will be utilized as an efficient tool for modeling and analyzing connectivity and spectrum allocation patterns of the multi-UAV network within a given area.
- For addressing the optimization intricacies inherent in the proposed graph coloring, sequential quadratic programming (SQP) [10] will be proposed to find the sub-optimal solution iteratively. SQP is chosen for its iterative optimization approach, which is well-suited for nonlinear programming problems (NLP), accuracy, and stability [11], [12], [13]. SQP has been applied in various research in wireless communication systems for small-cell networks [11], cognitive radio systems [12], V2V communication [13], etc. The algorithm's convergence and efficiency make it a good choice for optimizing spectrum resources among the interconnected UAVs, contributing to improved spectrum efficiency.
- For UAVs power control, $\mathcal{M}$-matrix theory, known for its optimality and computational efficiency, will be utilized as a powerful method for effective UAVs power control [14]. Its flexibility allows modeling of diverse system configurations, optimizing transmit powers of multi-UAVs while maintaining minimum link qualities.
- Numerical analyses are conducted to substantiate the efficiency of the proposed approach, revealing substantial improvements in both data rate and energy efficiencies when compared to other benchmark schemes.

The subsequent sections of this paper are organized as follows: Section II provides an overview of related works, Section III introduces the system model and formulates the problem, Section IV outlines the proposed approach for bandwidth allocation and power control optimization, Section V discusses the results and offers a detailed analysis, and, finally, conclusions in the last section, summarizes the key findings and implications of the proposed approach.

II. RELATED WORKS

Recently, there was a significant development in multi-UAVs research in wireless communication networks, focusing on various applications and key contributions. The highlighted studies include topics such as multi-UAV enabled mobile-edge computing for IoT networks [15], cooperative control strategies for multi-UAV formation keeping [16], federated learning-assisted multi-UAV networks in image classification scenarios [17], multi-agent deep reinforcement learning for trajectory optimization [18], joint communication and trajectory optimization for mobile internet of vehicles (IoVs) [19], efficient and secure multi-UAV communication via a secured UAV (S-UAV) model [20], and a clustering strategy to enhance security in multi-UAV flight formations [21]. These works collectively showcase advancements in optimizing communication, coordination, security, and computational efficiency in the evolving field of multi-UAV systems.

For multi-UAV spectrum allocation and power control optimization, which is the main focus of this paper, there are some research works studied them in [17], [18], [19], and [20]. The authors in [17] studied multi-UAVs and cellular base stations (BSs) within IoT framework, emphasizing uplink channel modeling. Introducing a binary exponential power control algorithm tailored for 5G networked UAV transmitters, the research considered 3D distance and multi-UAV reflections in the channel model. Simulations assessed the algorithm's impact on coverage probability, spectrum efficiency, and energy efficiency under various 3D distances. While this work prioritized power control initially and subsequently improved related parameters, our approach focuses on maximizing spectrum allocation first, followed by power control for multi-UAV networks. This strategy ensures UAVs receive the necessary data rate without unnecessary losses, subsequently contributing to spectrum utilization improvement. This step strategy not only ensures efficient data transmission but also minimizes the required power of UAVs, a facet not explored in the referenced work. The authors in [18] conducted a study aimed at enhancing resource allocation and addressing power control challenges within multi-UAV formation flight

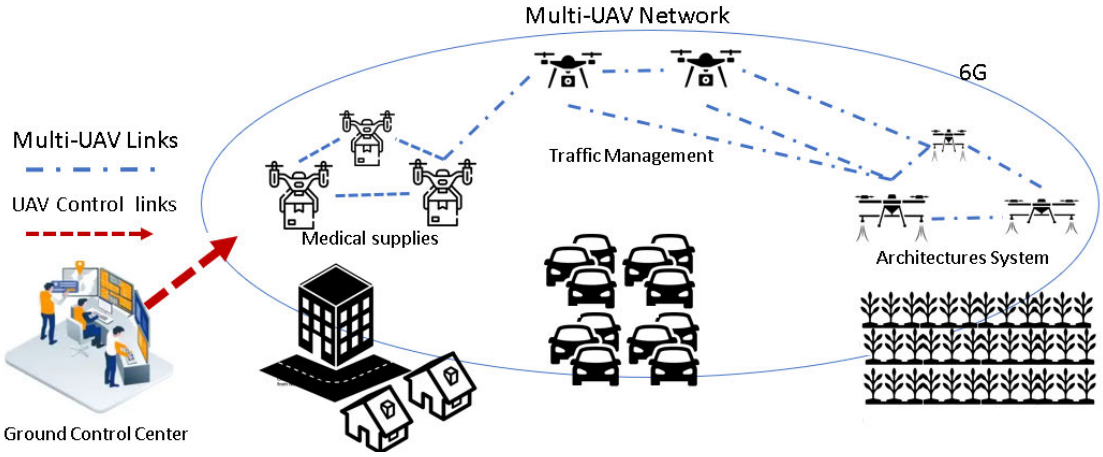

FIGURE 1. Provide an overview of a versatile multi-UAV network system, illustrating its capability to simultaneously engage in diverse applications. The network is adeptly controlled by ground control systems, showcasing the flexibility and adaptability of the multi-UAV setup. This integrated system has the potential to serve various purposes concurrently, demonstrating its efficiency in managing different tasks. The network's responsiveness to ground control systems ensures seamless coordination, making it a dynamic and multifunctional solution for a wide range of applications, all within a unified and controllable framework.

system engaged in radar sensing. It formulates a complex optimization problem to maximize the minimum signal-to-interference-plus-noise ratio (SINR) of radar echo signals, demonstrating its NP-hardness nature. The proposed iterative channel allocation and power control algorithm (ICAPCA), coupled with a reduced-complexity greedy channel allocation algorithm (GCAA), effectively addressed this problem, significantly enhancing minimum SINR and radar sensing performance compared to conventional methods. In contrast, our proposed approach aims at maximizing bandwidth allocations for all multi-UAVs, contributing to the comprehensive optimization of spectrum utilization. Notably, our work operates in 3D space, providing more accurate distance considerations, and differs in UAV distribution, influencing SINR values. The authors in [19] proposed a hierarchical multi-agent Q-learning framework for optimal frequency reuse and transmit power control in multi-UAV wireless networks, aiming to improve spectrum efficiency and equipment utilization. However, our work distinction lies in its comprehensive approach to jointly optimizing channel allocation and transmit power for enhanced network efficiency. The authors in [20] worked on meeting the requirements of high average spectral efficiency and maximizing the minimum average energy in multi-UAV formation communication, focusing on resource optimization using Deep Q-network. The paper emphasized the intelligent choice of power and frequency by UAVs based on remaining time and the number of UAVs in the formation. However, it does not explicitly highlight specific details or optimization techniques related to power control. In [22], using cell-free massive multiple-input multiple-output (mMIMO) for UAV communications, wireless power transfer (WPT) was incorporated to support both uplink data and pilot transmission. The research explores novel closed-form expressions considering UAV hardware impairments, showing significant uplink spectral efficiency (SE) improvements compared to current small cell (SC) and cellular massive MIMO systems. However, this work neither considered bandwidth allocation nor power control in multi-UAV networks. In [23], the utilization of cell-free mMIMO systems in mobile communications was examined, addressing deployment architectures, challenges, and innovative solutions such as predictor antennas, hierarchical cancellation, rate-splitting, and dynamic clustering. It also outlines future research directions to advance mobile cell-free massive MIMO communication technologies. Also, the problem of multi-UAV networking was not considered.

Consequently, the existing literature on multi-UAV network exhibit strengths, whereas faces limitations that the proposed method aims to overcome. The fact is that most of these studies considered a sequential optimization approach, addressing energy consumption first and then enhancing its related parameters, which leads to suboptimal outcomes. On the other hand, our proposed approach prioritizes maximizing spectrum allocations before refining power control. Thus, our proposal addresses these gaps by providing a detailed and comprehensive strategy for joint spectrum allocation and power control optimization in the multi-UAV networks.

III. PROPOSED SYSTEM MODEL

Figure 1 shows the proposed multi-UAV network architecture, where multiple UAVs are deployed to provide communication services to users in remote and hard-to reach areas. The system model consists of several UAVs hovering at an altitude of h, with a maximum number of M UAVs represented as $(v_1, v_2, v_3, \ldots, v_M)$. In this scenario, UAV channel allocation and power control are highly needed to maximize both spectrum and energy efficiencies of the overall network based on multi-UAV connection and data traffic in the UAV-to-UAV links. In this section, UAV-to-UAV channel

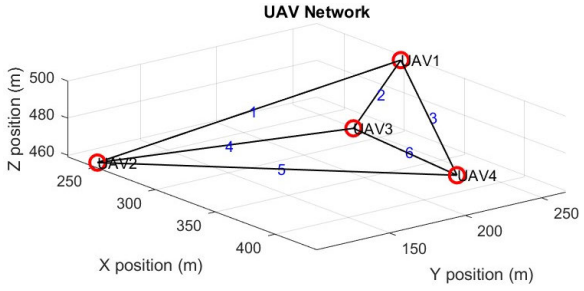

FIGURE 2. Provides a succinct visualization of a fully connected multi-UAV network system represented as a graph $G(V, E)$. Each UAV V is depicted as a vertex in the graph, and edges E signify direct communication links among UAVs, forming a comprehensive and interconnected network structure. This illustration offers a quick and clear overview of the extensive communication possibilities within the multi-UAV system.

model and the optimization problem formulation will be given.

A. UAV TO UAV CHANNEL MODEL

In the proposed model, the locations of UAVs are denoted by x_i, y_i and $z_i \in R^+$, where each UAV i, $1 \leq i \leq M$ is spatially defined by its coordinates within the 3D space, represented by Fig. 2. The separation distance d_{ij} between UAV i and UAV j is determined based on their 3D inter-distances as follows [15]:

$$d_{ij} = \sqrt{\left(d_{ij}^{Hr}\right)^2 + \left(d_{ij}^{Vt}\right)^2} \tag{1}$$

where d_{ij}^{Hr} is the horizontal distance between the projected locations of UAV i and UAV j. Also, d_{ij}^{Vt} is defined as the vertical distance between their projected locations. For UAV-to-UAV channel modeling, the Air–to–Air (A2A) channel modeling given in [16] will be utilized in this paper. In this modeling, only line-of-sight (LoS) links, characterized by an unobstructed path between the transmitter (Tx) and receiver (Rx), are a notable type [16], while non-LoS (NLoS) links rarely occurred and were not considered. Thus, the path loss of the LoS in the link L_{ij} between UAV i and UAV j is modeled as follows:

$$PL_{ij}^{LoS}[dB] = PL\left(d_0\right) + 10\alpha log_{10}\left(\frac{d_{ij}}{d_0}\right), \tag{2}$$

where PL_{ij}^{LoS} depends on the separation distance d_{ij}, its value at a reference distance d_0, i.e., $PL\left(d_0\right)$, and the path loss exponent α. The parameter d_0 is crucial in characterizing how the signal strength attenuates with increasing distance between the Tx and Rx in the communication link. The Tx power of a UAV, denoted as Pt_i, signifies the intensity of the signal it emits during communication. The Rx signal power, denoted as Pr_j in dB, is determined by adding Pt_i in dB with the path loss PL_{ij}^{LoS} as follows.

$$Pr_{ij}[dB] = Pt_i[dB] - PL_{ij}^{LoS}[dB], \tag{3}$$

SINR between Rx UAV j and Tx UAV i is crucial for evaluating the communication quality in the context of multi-UAV networks. This SINR, denoted as $SINR_{ij}$, is written as:

$$SINR_{ij} = \frac{Pr_{ij}}{\sum_{v=1, v\neq i}^{M} Pr_{vj} + \rho_0} \tag{4}$$

where Pr_{vj}, is Rx power at UAV j from Tx UAV v where $v \neq i$. In (4), the term $\left(\sum_{v=1, v\neq i}^{M} Pr_{vj}\right)$ represents the sum of interference powers, while ρ_0 represents the additive white gaussian noise (AWGN) power. Subsequently, the spectrum efficiency R_{ij} in bps/Hz is calculated as follows:

$$R_{ij} = log_2\left(1 + SINR_{ij}\right) \tag{5}$$

B. OPTIMIZATION PROBLEM FORMULATION

In this section, we will formulate the optimization problem of spectrum and power allocation for multi-UAV networks. The aim of the optimization problem is to maximize the overall data rate of the pre-connected multi-UAV network subject to the limited total bandwidth available for the network and UAVs maximum Tx powers, as follows:

$$\max_{B_{ij} Pt_i} \sum_{i=1}^{M} \sum_{j=1}^{M} \eta_{ij} B_{ij} R_{ij} \tag{6}$$

$$\text{s.t.} \quad \eta_{ij} \in (0, 1) \tag{6.a}$$

$$\sum_{i=1}^{M} \sum_{j=1}^{M} \eta_{ij} B_{ij} = B_{tot} \tag{6.b}$$

$$Pt_i \in (0, P_{tmax}) \tag{6.c}$$

where η_{ij} is the connection index which is equal to one if UAV i is connected to UAV j and zero otherwise. In this paper, η_{ij} is assumed to be pre-assigned based on the multi-UAV network architecture. The optimization of η_{ij} based on a certain objective function is out of the scope of this paper. B_{ij}, is the bandwidth allocated for UAV i and UAV j communication link, and B_{tot} is the total available bandwidth for the multi-UAV network. The second constraint given in (6.b) means that the sum of all bandwidths for all UAV-UAV links in the network should be equal to B_{tot}. The third constraint given in (6.c) indicates that the Tx power of UAV i should be bounded by its maximum Tx power P_{tmax}.

IV. PROPOSED APPROACH FOR BANDWIDTH ALLOCATION AND POWER CONTROL

The optimization problem given in (6) is an NLP due to its non-linear objective function. In this paper, to efficiently address it within its constraints, we will split it into two sub-problems. In the first sub-problem, B_{ij} optimization is conducted while considering all UAVs transmit at their maximum Tx power, i.e., $Pt_i = P_{tmax}$, while in the second sub-problem, Pt_is are adjusted based on the pre-adjusted B_{ij}.

A. GRAPH BASED BANDWIDTH OPTIMIZATION

Herein, graph theory using coloring graph is used to optimize the bandwidth allocations of the multi-UAV network while considering fixed maximum power allocation. In the context of a multi-UAV network shown in Fig. 2, it can be formally represented as a graph $G(V, E)$ where V denotes

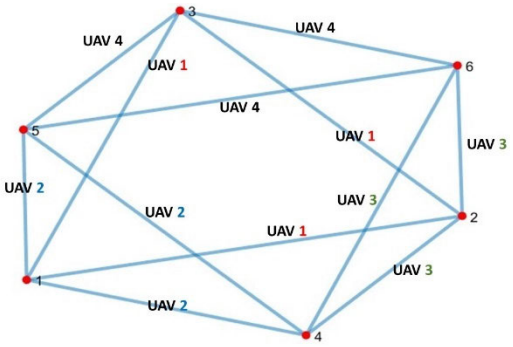

FIGURE 3. Provides an overview of a multi-UAV network system as corresponding link graph theory $\hat{G}(\hat{V}, \hat{E})$. The number of nodes in graph $\hat{G}(\hat{V}, \hat{E})$ corresponds to the number of links in the original graph $G(V, E)$.

the set of UAVs, and E represents the set of links among them. Correspondingly, the link graph $\hat{G}(\hat{V}, \hat{E})$ is derived based on the UAV entities and their connections as shown in Fig. 3. In this link graph, the edges in $G(V, E)$ given in Fig. 2, i.e., the channel links among UAVs, become the vertices in $\hat{G}(\hat{V}, \hat{E})$, and the vertices in $G(V, E)$, i.e., UAVs nodes, become the edges in $\hat{G}(\hat{V}, \hat{E})$. Thus, the number of nodes in the link graph $\hat{G}(\hat{V}, \hat{E})$ in Fig. 3, matches to the number of links in the original graph $G(V, E)$ in Fig. 2. This relationship between the number of nodes and links underscores the significance of the link graph representation in providing a condensed yet comprehensive view of the network connectivity. By leveraging link graph theory, we can simplify the visualization and analysis of network properties and optimization algorithms, ultimately facilitating a deeper understanding of the multi-UAV network system. In the overall link graph representation $\hat{G}(\hat{V}, \hat{E})$ of the multi-UAV network, let $\eta_{k(ij)} \in (0, 1)$ indicates the connection index of vertex k in $\hat{G}$ between UAVs i and j in graph G. Also, let $R_{k(ij)}$ represents its associated spectrum efficiency when UAV i transmits to UAV j in graph G. For example, vertex one in $\hat{G}$, i.e., $k = 1$, is used to connect UAV 1 and UAV 2 in G, see Figs. 2 and 3. Thus, the total spectrum efficiency of vertex k will be:

$$R_k = R_{k(ij)} + R_{k(ji)} \tag{7}$$

Also, let g_k be the percentage of the system's traffic injected by vertex k assuming UAVs have full buffer traffic loads. Thus, g_k is only influenced by the spectrum efficiency of link k, and can be evaluated as follows:

$$g_k = \frac{R_k}{\sum_{l=1}^{K} R_l} \tag{8}$$

In this scenario, B_{tot} needs to be collectively shared among all vertices in graph $\hat{G}$. In G, edges that do not interfere with each other have the capability to reuse the same bandwidth [21]. Consequently, the corresponding vertices in $\hat{G}$ can efficiently share and reuse the same bandwidth. Based on graph representation, achieving optimal spectrum efficiency necessitates the formulation of a suitable optimization problem, encompassing an appropriate objective function and constraints. The initial step involves defining constraints, particularly those related to frequency reuse, with quantitative precision. To do that, we refer to a crucial definition from graph theory:

Definition 1: An independent set in a graph $\hat{G}(\hat{V}, \hat{E})$ constitutes a subset of the vertex set $\hat{V}$ such that no two vertices in V share an edge between them. A maximal independent set (MIS) of $\hat{G}$ is an independent set that is not a proper subset of another independent set in $\hat{G}$ [24].

The MIS, in the context of $\hat{G}$, identifies sets of vertices that can effectively reuse the same bandwidth. Suppose that graph $\hat{G}$ contains Q such MIS. Let an MIS represents a matrix of size $(Q \times K)$ that systematically conveys information about each vertex's membership in various MISs as follows:

$$MIS = \begin{bmatrix} s_{11} & s_{12} & \cdots & s_{1K} \\ s_{21} & s_{22} & \cdots & s_{2K} \\ \vdots & \vdots & \ddots & \vdots \\ s_{Q1} & s_{Q2} & \cdots & s_{QK} \end{bmatrix} \tag{9}$$

where, the elements of the MIS matrix, s_{qk}, indicates whether vertex k belong to MIS q or not, as follows:

$$s_{qk} = \begin{cases} 1 & \textit{Vertix } k \textit{ belongs to MIS } q \\ 0 & \textit{otherwise} \end{cases} \tag{10}$$

Let the variable X_q denotes the bandwidth assigned to all vertices within the MIS q. This representation significant is that all vertices belonging to a specific MIS can collectively utilize the same allocated bandwidth. By considering MISs and constant power allocation, the optimization problem given in (6) can be re-written as follows:

$$\max_{X_q} \sum_{k=1}^{K} \sum_{q=1}^{Q} X_q s_{qk} \tag{11}$$

$$\text{s.t.} \quad \eta_k \in (0, 1) \quad \forall i, j \in k \tag{11.a}$$

$$[s_{kq}] \in (0, 1) \tag{11.b}$$

$$g_k \leq 1, \forall k \tag{11.c}$$

$$\sum_{k=1}^{K} g_k = 1 \tag{11.d}$$

$$\sum_{q=1}^{Q} X_q = B_{tot} \tag{11.e}$$

$$\sum_{q=1}^{Q} X_q s_{kq} \geq B_{tot} g_k, \ \forall \eta_k = 1 \tag{11.f}$$

This optimization problem aims to maximize the weighted sum of MISs bandwidth allocations X_q subject to various constraints. The first constraint given in (11.a) is the same as that given in (6.a), which indicates the connection status of vertex k connecting UAV i and UAV j. The second constraint given in (11.b) indicates that the element s_{kq} can be either 0 or 1 based on the MIS structure. The third and the fourth constraints given in (11.c) and (11.d) respectively, bound the value of g_k to be less than or equal to 1, and their summation $\forall k$ should be equal 1. The fifth constraint given in (11.e) indicates that the total bandwidths assigned to all MISs should be equal to B_{tot}. The sixth constraint

given in (11.f) indicates that the bandwidth assigned to an established vertex k from all its designated MISs should be greater than or equal to its percentage of the total injected system traffic.

To solve the NLP problem given in (11), nonlinear optimization techniques such as SQP method can be utilized. SQP is an iterative algorithm that aims to find the optimal solution by iteratively updating the decision variable using a sequence of quadratic subproblems. Each of these subproblems serves as an approximation to the original nonlinear optimization problem. The objective is to find an optimal solution by refining the approximation in each iteration. The algorithm begins with an initialization step, by randomly selecting a feasible starting solution of the vector $\boldsymbol{X}_q^{\omega} = [X_1^{\omega}, X_2^{\omega}, \ldots X_Q^{\omega}]$, i.e., $\boldsymbol{X}_q^0$ at $\omega = 0$, where ω indicates the iteration number. Then, the objective function $f\left(\boldsymbol{X}_q^{\omega}\right)$ will be written as given in (12) to iteratively solve (11). The constraints of $f\left(\boldsymbol{X}_q^{\omega}\right)$, i.e., $\mathrm{c}\left(\boldsymbol{X}_q^{\omega}\right)$ and $\mathrm{h}\left(\boldsymbol{X}_q^{\omega}\right)$, which are defined in (13) and (14), respectively, ensure the satisfaction of the main constraints given in (11.e) and (11.f) at each iteration ω.

$$f\left(\boldsymbol{X}_q^{\omega}\right) = \sum_{k=1}^{K} \sum_{q=1}^{Q} X_q^{\omega} s_{qk} \tag{12}$$

$$c\left(\boldsymbol{X}_q^{\omega}\right) = \sum_{q=1}^{Q} X_q^{\omega} - B_{tot} = 0 \tag{13}$$

$$h\left(\boldsymbol{X}_q^{\omega}\right) = \sum_{q=1}^{Q} X_q^{\omega} s_{kq} - B_{tot} g_k \geq 0 \tag{14}$$

Then, at each iteration ω, the aim is to solve the following quadratic equation iteratively:

$$\min \boldsymbol{\beta}_w \left[\nabla f\left(\boldsymbol{X}_q^{\omega}\right)^T \boldsymbol{\beta}_{\omega} + \frac{1}{2} \boldsymbol{\beta}_{\omega}^{\mathrm{T}} \nabla^2 L(\boldsymbol{X}_q^{\omega}, \lambda_{\omega}, \mu_{\omega}) \boldsymbol{\beta}_{\omega} \right] \tag{15}$$

$$\text{s.t.} \quad c\left(\boldsymbol{X}_q^{\omega}\right) + \nabla \mathrm{c}\left(\boldsymbol{X}_q^{\omega}\right)^T \boldsymbol{\beta}_{\omega} = 0 \tag{15.a}$$

$$h\left(\boldsymbol{X}_q^{\omega}\right) + \nabla h\left(\boldsymbol{X}_q^{\omega}\right)^T \boldsymbol{\beta}_{\omega} \geq 0 \tag{15.b}$$

where $\mathcal{L}(\boldsymbol{X}_q^{\omega}, \lambda_{\omega}, \mu_{\omega})$ indicates the Lagrangian function at an iteration ω, which is defined as follows:

$$\mathcal{L}\left(\boldsymbol{X}_q^{\omega}, \lambda_{\omega}, \mu_{\omega}\right) = f\left(\boldsymbol{X}_q^{\omega}\right) + \lambda_{\omega} c\left(\boldsymbol{X}_q^{\omega}\right) + \mu_{\omega} h\left(\boldsymbol{X}_q^{\omega}\right) \tag{16}$$

Thus, $\boldsymbol{\beta}_{\omega}$ denotes the increment vector of the decision variable $\boldsymbol{X}_q^{\omega}$ and the Lagrangian multiplies λ_{ω} and μ_{ω}, as follows:

$$\boldsymbol{\beta}_{\omega} = [(\boldsymbol{X}_q^{\omega+1} - \boldsymbol{X}_q^{\omega}), (\lambda_{\omega+1} - \lambda_{\omega}), (\mu_{\omega+1} - \mu_{\omega})]^T, \tag{17}$$

where T indicates the transpose operation. In (15) $\nabla f\left(\boldsymbol{X}_q^{\omega}\right)^T$, $\nabla \mathrm{c}\left(\boldsymbol{X}_q^{\omega}\right)^T$, and $\nabla h\left(\boldsymbol{X}_q^{\omega}\right)^T$ are the transposes of the vectors containing the first derivative of the objective function and the constraints stated in (12), (13), and (14), respectively, with respect to $\boldsymbol{X}_q^{\omega}$. Also, $\nabla^2 \mathcal{L}(\boldsymbol{X}_q^{\omega}, \lambda_{\omega}, \mu_{\omega})$ is the hessian of the Lagrangian function with respect to $\boldsymbol{X}_q^{\omega}$, which can be expressed as follows:

$$\nabla^2 \mathcal{L}\left(\boldsymbol{X}_q^{\omega}, \lambda_{\omega}, \mu_{\omega}\right) = \begin{bmatrix} \frac{\partial^2 \mathcal{L}}{\partial (X_1^{\omega})^2} & \frac{\partial^2 \mathcal{L}}{\partial X_1^{\omega} \partial X_2^{\omega}} & \cdots & \frac{\partial^2 \mathcal{L}}{\partial X_1^{\omega} \partial X_Q^{\omega}} \\ \frac{\partial^2 \mathcal{L}}{\partial X_2^{\omega} \partial X_1^{\omega}} & \frac{\partial^2 \mathcal{L}}{\partial (X_2^{\omega})^2} & \cdots & \frac{\partial^2 \mathcal{L}}{\partial X_2^{\omega} \partial X_Q^{\omega}} \\ \vdots & \vdots & \ddots & \vdots \\ \frac{\partial^2 \mathcal{L}}{\partial X_Q^{\omega} \partial X_1^{\omega}} & \frac{\partial^2 \mathcal{L}}{\partial X_Q^{\omega} \partial X_1^{\omega}} & \cdots & \frac{\partial^2 \mathcal{L}}{\partial \left(X_Q^{\omega}\right)^2} \end{bmatrix}, \tag{18}$$

Solving this optimization problem yields the optimal values of $\boldsymbol{\beta}_{\omega}$, which is used to find the values of $\boldsymbol{X}_q^{\omega+1}$, $\lambda_{\omega+1}$ and $\mu_{\omega+1}$ using (17).

Algorithm 1 outlines the proposed SQP approach to sequentially optimize the $\boldsymbol{X}_q$. The inputs to the algorithm are the MIS structure s_{qk}, the total available bandwidth B_{tot}, the network topology including η_k and g_k, the total number of iterations N_{it} and the convergence threshold δ. For initialization, an initial guess for $\boldsymbol{X}_q^0$ at iteration $\omega = 0$ is randomly initialized. Then during the algorithm and while $\omega \leq N_{it}$, the values of $f\left(\boldsymbol{X}_q^{\omega}\right)$, $\mathrm{c}\left(\boldsymbol{X}_q^{\omega}\right)$, and $h\left(\boldsymbol{X}_q^{\omega}\right)$ are evaluated using (12), (13) and (14), respectively. Lagrangian function given in (16) is formulated and the $\nabla^2 \mathcal{L}\left(\boldsymbol{X}_q^{\omega}, \lambda_{\omega}, \mu_{\omega}\right)$ is calculated using (18). Then, the quadratic optimization given in (15) is solved and $\boldsymbol{\beta}_{\omega}$ is obtained. Afterwards, the values of $\boldsymbol{X}_q^{\omega+1}$, $\lambda_{\omega+1}$, and $\mu_{\omega+1}$ are evaluated using (17). Then the optimal values of $\boldsymbol{X}_q^*$ are set equal to $\boldsymbol{X}_q^{\omega+1}$. The convergence threshold is tested to decide whether to terminate the algorithm or continue till $\omega = N_{it}$, where the minimum square error (MSE) between $\boldsymbol{X}_q^{\omega+1}$ and $\boldsymbol{X}_q^{\omega}$ is calculated and compared with δ as given in Algorithm 1. Then, the value of ω is incremented by one.

Algorithm 1 Proposed SQP for $\boldsymbol{X}_q^*$ Optimization

Output: $\boldsymbol{X}_q^*$
Input: $s_{qk}, B_{tot}, \eta_k, g_k, N_{it}$, and δ
Initialize: $\boldsymbol{X}_q^0 \leftarrow$ initialguessat$\omega = 0$
While $\omega \leq N_{it}$
1. Evaluate: $f\left(\boldsymbol{X}_q^{\omega}\right)$, $\mathrm{c}\left(\boldsymbol{X}_q^{\omega}\right)$, and $h\left(\boldsymbol{X}_q^{\omega}\right)$ using (12), (13) and (14)
   Formulate: $\mathcal{L}\left(\boldsymbol{X}_q^{\omega}, \lambda_{\omega}, \mu_{\omega}\right)$ using (16)
2. **Calculate:** $\nabla^2 \mathcal{L}\left(\boldsymbol{X}_q^{\omega}, \lambda_{\omega}, \mu_{\omega}\right)$ using (18)
3. **Solve:**The quadratic subproblem given in (15) and then obtain $\boldsymbol{\beta}_{\omega}$
4. **Calculate:** $\boldsymbol{X}_q^{\omega+1}$, $\lambda_{\omega+1}$, and $\mu_{\omega+1}$ using (17)
5. **Set** $\boldsymbol{X}_q^* = \boldsymbol{X}_q^{\omega+1}$
6. **If** $\frac{1}{Q} \sum_{q=1}^{Q} \left(X_q^{\omega+1} - X_q^{\omega+1}\right)^2 \leq \delta$
   Break **While**
   End If
7. $\omega = \omega + 1$

End While

B. MULTI-UAVS POWER CONTROL USING $\mathcal{M}$-MATRIX

After optimizing B_k^* of each vertex k based on the optimized bandwidths of its related MISs, power allocations of its corresponding UAVs i and j are adjusted. The goal is to minimize the total UAVs Tx powers while satisfying the optimized data rates of their associated links.This maximizes the systems' energy efficiency in consequence. Additionally, power control leads to reduced interference among UAVs. In this context, we will utilize the $\mathcal{M}$-matrix theory to optimize the UAVs' Tx powers [26]. To do that, we transfer back from the link graph $\hat{G}$ given in Fig. 3 to the original node graph G given in Fig. 2. This shift is necessitated by the fact that bandwidth is assigned to links, while power is transmitted by devices. Thus, the power optimization sub-problem can be formulated as follows:

$$\min_{pt_i} \sum_{i=1}^{M} Pt_i, \tag{19}$$

$$\text{s.t.} \quad Pt_i \in (0, P_{tmax}), \forall i \in M, \tag{19.a}$$

$$\frac{Pt_i \left|h_{ij}\right|^2}{\sum_{v=1.v\neq i}^{M} Pt_v \left|h_{vj}\right|^2 + \rho_0} \geq \varphi_k^* \ \forall i,j \in k \tag{19.b}$$

where $\varphi_k^* = \left(2^{c_k/B_k^*} - 1\right)$ is the adjusted SINR of the link k connecting UAV i and UAV j. Herein, c_k is the minimum data rate requirement in bps of link k using its adjusted B_k^* coming from the SQP algorithm. $\left|h_{ij}\right|^2$ is the channel gain between UAV i and UAV j, while $\left|h_{vj}\right|^2$ is the channel gain between UAV v, $v \neq i$, and UAV j. Both can be calculated using the path loss equation given in (2). The first constraint given in (19.a) is the same as that given in constraint (6.c) of the original problem. The second constraint given in (19.b) indicates that the minimum $SINR_{ij}$ of the link k connecting UAVs i and j is bounded by its φ_k^* value. This ensures that the power control algorithm should satisfy the minimum channel quality level among UAVs. Using convex optimization, constraint (19.b) can be relaxed as $\frac{Pt_i\left|h_{ij}\right|^2}{\sum_{v=1.v\neq i}^{M} Pt_v\left|h_{vj}\right|^2+\rho_0} = \varphi_k^*$ and then the energy efficiency is maximized. Thus, the power control can be solved as a set of linear equations.

$$\frac{Pt_i \left|h_{ij}\right|^2}{\varphi_k^*} - \sum_{v=1.v\neq i}^{M} Pt_v \left|h_{vj}\right|^2 = \rho_0, \tag{20}$$

which can be expressed using matrix-vector notation as follows:

$$\boldsymbol{A}_i \boldsymbol{P}t_i = \boldsymbol{w} \Rightarrow \boldsymbol{P}t_i = \boldsymbol{A}_i^{-1}\boldsymbol{w}, \tag{21}$$

where

$$\boldsymbol{A}_i = \begin{pmatrix} \left|h_{1j}\right|^2 / \varphi_k^* & -\left|h_{2j}\right|^2 & \cdots & -\left|h_{Mj}\right|^2 \\ -\left|h_{1j}\right|^2 & \left|h_{2j}\right|^2 / \varphi_k^* & \cdots & -\left|h_{Mj}\right|^2 \\ \vdots & \vdots & \ddots & \vdots \\ -\left|h_{1j}\right|^2 & -\left|h_{2j}\right|^2 & \cdots & \left|h_{Mj}\right|^2 / \varphi_k^* \end{pmatrix} \tag{22}$$

$$\boldsymbol{P}t_i = \begin{pmatrix} Pt_1 \\ Pt_2 \\ Pt_3 \\ \vdots \\ Pt_M \end{pmatrix} \text{ and } \boldsymbol{w} = \rho_0 \begin{pmatrix} 1 \\ 1 \\ 1 \\ \vdots \\ 1 \end{pmatrix} \tag{23}$$

It is important to mention that the matrix $\boldsymbol{A}_i$, which has a dimension of $M \times M$, is considered a $\mathcal{Z}$-matrix, following the description given in [23] and [24]. In other words, it is a matrix where all off-diagonal elements are less than or equal to zero. In order to find the solution for $\boldsymbol{P}t_i$, it is necessary for $\boldsymbol{A}_i$ to be also an $\mathcal{M}$ -matrix. An $\mathcal{M}$ -matrix is a special type of $\mathcal{Z}$-matrix whose inverse consists of all nonnegative elements. Thus, to solve equation (21) and obtain $\boldsymbol{A}_i^{-1}$, we will apply the Sherman-Morrison formula given in [26]. To facilitate this, we will re-express $\boldsymbol{A}_i$ as follows:

$$\boldsymbol{A}_i = \boldsymbol{F}_i - \boldsymbol{1}_M \Delta_i^T \tag{24}$$

where

$$\boldsymbol{F}_i = \text{diag}\left(h_{ij}\left[\frac{1}{\varphi_k^*} + 1\right]\right), 1 \leq j \leq M$$

$$\boldsymbol{1}_M = \begin{pmatrix} 1 \\ 1 \\ 1 \\ \vdots \\ 1 \end{pmatrix}, \text{ and } \Delta_i^T = \begin{pmatrix} h_{1j} \\ h_{2j} \\ h_{3j} \\ \vdots \\ h_{Mj} \end{pmatrix}^T \tag{25}$$

The Sherman-Morrison theorem [26] provides a method to compute the inverse of any off-diagonal singular square matrix in the form of equation (24). This inverse is given by:

$$\boldsymbol{A}_i^{-1} = \boldsymbol{F}_i^{-1} + \frac{\boldsymbol{F}_i^{-1}\boldsymbol{1}_M \Delta_i^T \boldsymbol{F}_i^{-1}}{1 - \Delta_i^T \boldsymbol{F}_i^{-1}\boldsymbol{1}_M} \tag{26}$$

However, there is a crucial condition for finding a feasible non-negative solution for $\boldsymbol{P}t_i$ using equation (26), which is as follows:

$$\sum_{i=1}^{M} \left(1 + \frac{1}{\varphi_k^*}\right)^{-1} < 1 \tag{27}$$

The proof of this condition directly follows from equation (26), where $\boldsymbol{F}_i$, $\boldsymbol{1}_M$, and Δ_i^T are all positive diagonal matrices and vectors as depicted in equation (25). Therefore, from equation (26), $\boldsymbol{A}_i$ becomes an $\mathcal{M}$-matrix, meaning that $\boldsymbol{A}_i^{-1}$ contains only non-negative elements, if and only if the denominator if $1 - \Delta_i^T \boldsymbol{F}_i^{-1}\boldsymbol{1}_M > 0$ or $\Delta_i^T \boldsymbol{F}_i^{-1}\boldsymbol{1}_M < 1$. This leads to the condition in (27) using (25). However, it is important to note that the condition in (27) solely ensures the lower bound condition of $\boldsymbol{P}t_i$, which is $\boldsymbol{P}t_i \geq 0$, without addressing the upper bound condition, i.e., $\boldsymbol{P}t_i \leq P_{tmax}$. Therefore, the solution for $\boldsymbol{P}t_i$ obtained through (26) should be constrained by its maximum value, P_{tmax}. It is important to note that by reducing the UAVs Tx powers, we enable the neighboring links in the multi-UAV network to reuse the same bandwidth. This set influences the enhancement of spectrum efficiency as discussed in section A.

TABLE 1. Simulation parameters.

Symbol	Value
α	2.03 [16]
d_0	1 m [16]
$PL(d_0)$	46.4 [16]
d_{ij}^v	50 m[16]
d_{ij}^h	Randomly allocated in the range of [1,100] m [16]
B_{tot}	10 MHz [27]
P_{tmax}	1 Watt [28]
ρ_0	$-147 + 10\log_{10}(B) + 10$[28]

V. NUMERICAL RESULTS AND DISCUSSION

In this section, the performance of the proposed algorithms including coloring-graph based SQP and $\mathcal{M}$-matrix theory-based power control is assessed through extensive Monte-Carlo numerical simulations. The simulation area encompasses a post disaster area, where random number of UAVs are deployed in this area with arbitrarily horizontal distances in the range of [1,100] m, and the UAVs' vertical distance is adjusted to 50 m. The reference distance d_0 is set to 1 m, and the maximum UAVs' Tx powers are set to 1 watt. The total available bandwidth for the multi-UAV communication system is set to 10 MHz. Additional simulation parameters are listed in Table 1; unless otherwise stated. The performance of the proposed approach is evaluated by comparing it with three different benchmarks, which are the scheme given in [14], the maximum spectrum packing (MASPECT) algorithm given in [29], and the random selection (RS). In the scheme given in [14], a linear optimization problem using graph theory was formulated for bandwidth allocation in device to devices (D2D) network, accounting for link heterogeneity in demands and traffic injection patterns. The objective was to maximize the spectrum efficiency while efficiently utilizing the available bandwidth. In MASPECT algorithm given in [29], a distributed opportunistic channel acquisition mechanism for improving spectrum utilization was proposed using graph theoretic approach. In RS both bandwidth and power resources are set randomly in the ranges of $[0, P_{tmax}]$ and $[0, B_{tot}]$, respectively. In the simulation scenarios, we generate random geometric graphs with graph densities of 0.5, 0.8 and 1, where a graph density of 1 means that the network is fully connected, where all UAVs are mutually connected and $\eta_{ij} = 1 \forall i, j$. For graph density of 0.8 (0.5), the number of UAVs mutual connections is 80% (50%) of that of the fully connected network using random η_{ij}.

Figures 4, 5 and 6 represent the data rate performances in Mbps of the schemes involved in the comparisons at fixed UAVs' Tx power of P_{tmax} and network densities of 1, 0.8, and 0.5, respectively. Generally, as the number of UAVs increases, the data rates of all compared schemes are decreasing in consequence. This is due to the increased interference level among the deployed UAVs, where the limited availability of bandwidth resources and fixed power allocation exacerbate the issue. That is, as the number of UAVs escalates, the bandwidth resources allocated per UAV diminish, resulting in reduced data rates for each individual UAV. Moreover, by comparing the results presented in Figs 4, 5 and 6, we can conclude that network density plays a crucial role

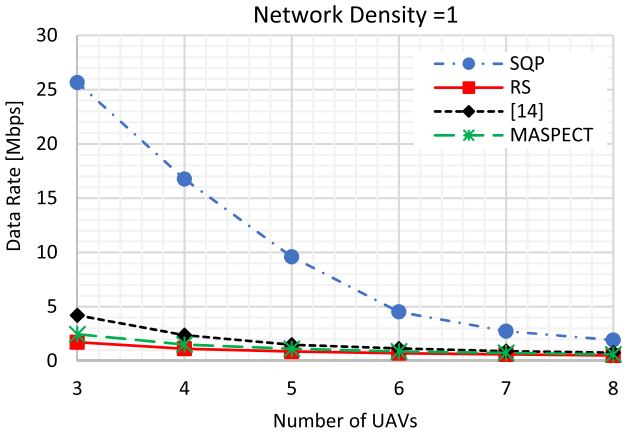

FIGURE 4. Data rate against the number of UAVs with network density = 1 and fixed power allocation.

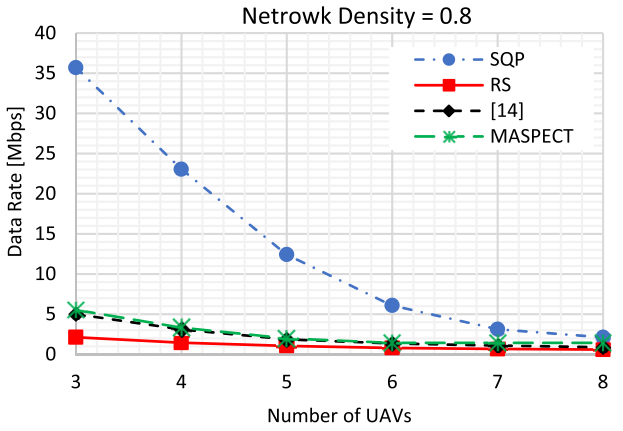

FIGURE 5. Data rate against the number of UAVs with network density = 0.8 and fixed power allocation.

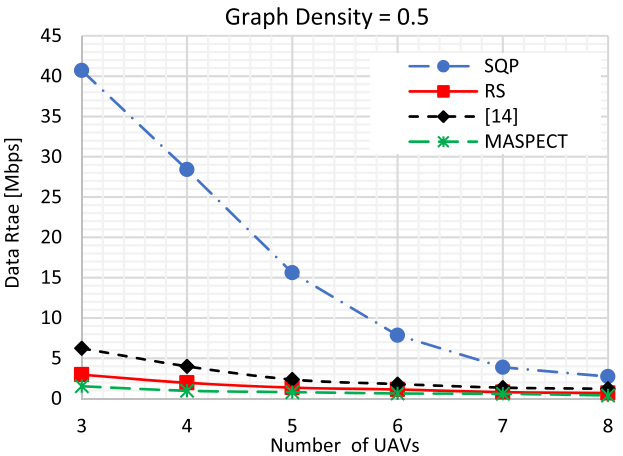

FIGURE 6. Data rate against the number of UAVs with network density = 0.5 and fixed power allocation.

in influencing data rate outcomes. When network density is low, the data rate tends to be high due to the less interference among the limited number of connected UAVs. This can be observed when comparing the data rates of graph density of 1 presented in Fig. 4, with those results from low density of 0.5 presented in Fig. 6, where a higher density results in lower data rate performance, and vice versa. This discrepancy can be attributed to the increased number of links, leading to elevated interference levels with a fixed power allocation. Thus, the juxtaposition of these scenarios underscores the intricate interplay between network density, interference, and link dynamics, ultimately influencing the overall data rate performance of the compared schemes.

Looking closer, the figures highlight that the proposed coloring-graph based SQP approach outperforms other methods in maximizing data rates. Notably, in Figs 4, 5 and 6, the proposed coloring-graph based SQP algorithm emerges as the standout performer, demonstrating a remarkable improvement of over 70% in data rate when the number of UAVs is set to 3 in all tested network densities. This substantial enhancement, however, exhibited diminishing returns as the number of UAVs increased, eventually converging to a difference of less than 10% compared to alternative methods due to excessive mutual interference. Also, UAVs' fixed Tx power allocation may lead to congestion and heightened interference, counteracting the potential benefits gained from the addition of more UAVs.

From Fig. 4 and when using 3 fully connected UAVs, i.e., network density of 1, RS yields the lowest data rate of approximately 1.72 Mbps. In contrast, MASPECT improves performance, achieving nearly 2.46 Mbps, while the scheme proposed in [14] excels further with a data rate of 4.21 Mbps. Notably, the proposed SQP algorithm stands out, surpassing all alternatives with an impressive data rate of approximately 25.6 Mbps. Shifting to scenarios with network density of 0.8, in Fig. 5 and using 3 UAVs, MASPECT becomes less favorable, yielding a data rate of 2.12 Mbps, while RS achieves a relatively higher data rate of 2.94 Mbps. The scheme proposed in [14] maintains commendable performance of approximately 5 Mbps, and the proposed SQP with coloring graph excels with a remarkable data rate of 36 Mbps, showcasing adaptability to varying network densities. Similarly, at a network density of 0.5 given in Fig. 6 and using 3 UAVs, MASPECT remains less favorable with a data rate of 1.5 Mbps, while RS achieves 2.96 Mbps. The schemes proposed in [14] reaches around 6.2 Mbps, and the proposed SQP with coloring graph excels with a data rate of 41 Mbps. The observed lower data rate of RS in a high-density network of 1 can be attributed to its random allocation mechanism, leading to increased interference in the densely connected UAVs. This unstructured allocation results in contention for bandwidth among UAVs, thereby diminishing the data rate. On the contrary, MASPECT by leveraging graph-based algorithms excels in a fully connected network by considering node degrees and probabilities, mitigating interference, and achieving a higher data rate compared to RS. The outstanding

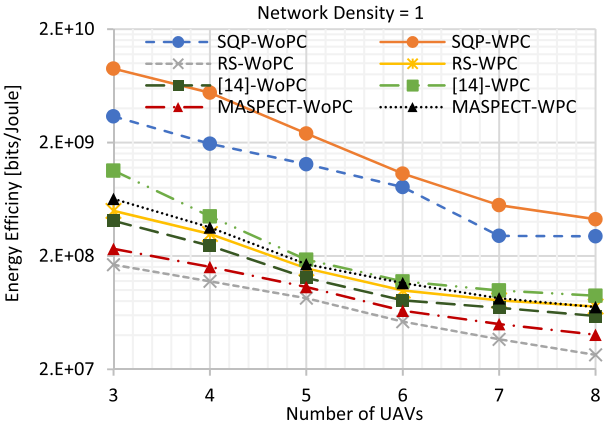

FIGURE 7. Energy efficacy against the number of UAVs with network density = 1 and with power control (WPC) and without power control (WoPC).

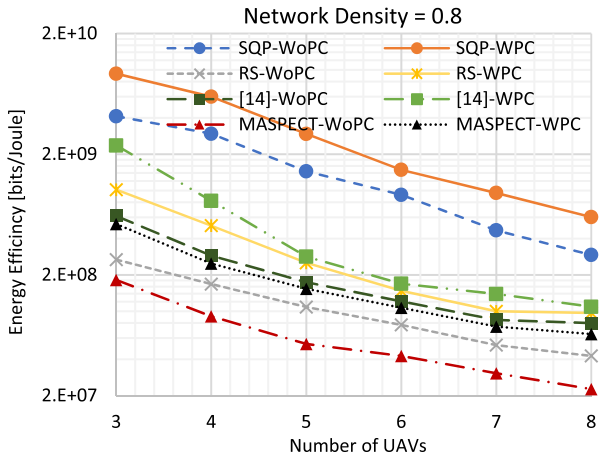

FIGURE 8. Energy efficacy against the number of UAVs with network density = 0.8 and with power control (WPC) and without power control (WoPC).

performance of the scheme given in [14] is owed to its linear optimization formulation, strategically allocating resources, and optimizing bandwidth in response to varying network conditions. It is interesting to note that at a network density of 0.5, the Rand scheme outperforms MASPET. This is because in less densely connected networks, RS's efficient random allocation allows for more effective bandwidth utilization. In contrast, MASPECT faces challenges as network density decreases as it impacts its ability to leverage the network topology for optimal bandwidth utilization.

Figures 7, 8, and 9 provide a comprehensive analysis of energy efficiency (EE) in (bits/Joule) in multi-UAV networks under different power control scenarios, i.e., with power control - WPC and without power control – WoPC, across varying network densities of 1, 0.8, and 0.5, respectively. The integration of power allocation, particularly employing $\mathcal{M}$-matrix theory, emerges as a standout performer in terms of EE, showcasing its superiority over fixed power allocation when integrated with the schemes involved in the comparison. Examining the results in Fig. 7 for a network density of 1 and fully connected 3 UAV, it becomes evident

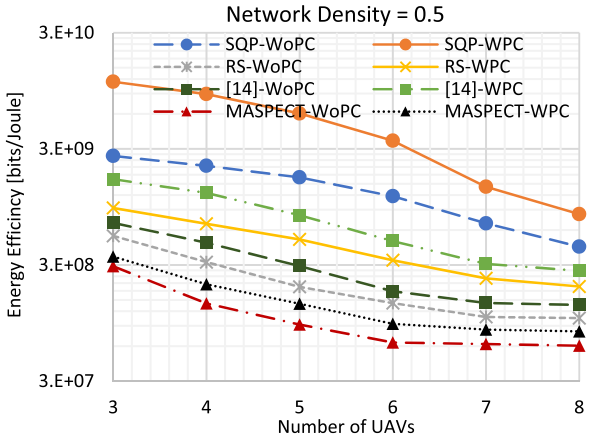

FIGURE 9. Energy efficacy against the number of UAVs with network density = 0.5 and with power control (WPC) and without power control (WoPC).

that the proposed SQP, particularly when complemented with the proposed power control strategy, achieves remarkable EE of approximately 9 Gbit/Joule. This stands in stark contrast to the significant 50% reduction observed without employing power control. The underlying reason behind this substantial improvement lies in the ability of power control to dynamically adapt power levels in response to evolving network conditions, minimizing total UAV transmission powers, and subsequently maximizing EE. Comparing EE across different methods, we observe that the EE of the proposed SQP WPC is notably higher at 9G bit/Joule, surpassing the EE of the method given in [14]-WPC at 1.13G bit/Joule. The EEs of MASPECT- WPC and RS-WPC are lower than that of [14]-WPC, achieving 0.637 Gbit/Joule and 0.5 Gbit/Joule, respectively. However, the worst-case scenario is observed in RS-WoPC, where EE is significantly low at 0.167 Gbit/Joule. Moreover, EEs of all schemes involved in the comparisons are decreasing with the increasing of the number of UAVs. This is owed to the decrease in their achievable data rates presented in Fig. 4 due to excessive interference. For example, EE of the proposed SQP-WPC falls from 9 Gbit/joule when using 3 fully connected UAVs to 0.42 Gbit/Joule when using 8 fully connected UAVs as shown in Fig .4.

In Fig. 8, the evaluation of EE across the compared schemes, each involving 3 UAVs and a graph density of 0.8, reveals distinct performances. The proposed SQP algorithm, when paired with power control, demonstrates exceptional EE, achieving around 9.3 Gbit/Joule. This underscores the SQP's efficiency in optimizing data rates while considering power consumption in the specified network scenario. SQP-WoPC maintains commendable EE at approximately 4.19 Gbit/Joule, where it is less than half the performance of QSP-WPC. The scheme [14]-WPC, achieves competitive EE at about 2.37 Gbit/Joule, while its non-power-controlled counterpart [14]-WoPC shows a notable reduction in EE at around 1.02 Gbit/Joule. RS-WPC and RS-WoPC, achieve EE values of approximately 0.619 Gbit/Joule and 0.268 Gbit/Joule, respectively, highlighting the impact of power control on EE improvement. MASPECT-WPC reaches an EE of approximately 0.528 Gbit/Joule, while MASPECT-WoPC exhibits the lowest EE among the methods, at around 0.182 Gbit/joule.

In Fig. 9 and using 3 UAVs, SQP-WPC stands out with a remarkable EE of nearly 11.4 Gbit/Joule, while SQP-WoPC maintains a low EE of 2.61 Gbit/Joule, further highlighting the significance of power control in enhancing performance. However, other methods exhibit lower EE values than the proposed SQP scheme, with [14]-WPC at 1.65 Gbit/Joule, RS-WPC at 0.93 Gbit/Joule, MASPECT-WPC at 0.355 Gbit/Joule. For WoPC, [14]-WoPC achieves 0.692 Gbit/Joule, RS-WoPC achieves 0.535 Gbit/Joule, and MASPECT-WoPC achieves 0.293 Gbit/Joule. These results underscore the pivotal role of power control, particularly in scenarios with lower graph density, in optimizing the EE of multi-UAV communication networks.

VI. CONCLUSION

This paper delves into the intricate challenges of bandwidth allocation and power control in multi- UAV networks. In this context, two stage optimization were proposed. In the first stage, bandwidth allocations were optimized by the means of coloring graph based SQP algorithm while considering fixed power allocations. In the second stage, $\mathcal{M}$-matrix theory was utilized to adjust the Tx powers of the UAVs based on their minimum data rate requirements using its adjusted bandwidth allocations done in the first stage. Through rigorous numerical simulations, our proposed approach demonstrated superior performance compared to other benchmarks for data rates maximization. Also, the proposed power control scheme demonstrated superior performances over fixed power allocation counterpart. This research contributes valuable insights into the realm of multi-UAV network optimization, paving the way for enhanced information transmission rates and resource utilization in dynamic and challenging environments. As the current study primarily focused on bandwidth allocation and power control, we only considered static scenarios, where UAVs are hovering at a fixed altitude above the earth's surface. Detailed exploration of network dynamics, including factors such as nodes mobility, traffic patterns, and topology changes, falls slightly outside the scope of the current paper, and it will be the subject of our future investigations. Also, optimizing communication delays against interference will be explored during our future studies.

REFERENCES

[1] E. M. Mohamed, M. Alnakhli, S. Hashima, and M. Abdel-Nasser, "Distribution of multi mmWave UAV mounted RIS using budget constraint multi-player MAB," *Electronics*, vol. 12, no. 1, p. 12, Dec. 2022, doi: 10.3390/electronics12010012.

[2] M. Mozaffari, X. Lin, and S. Hayes, "Toward 6G with connected sky: UAVs and beyond," *IEEE Commun. Mag.*, vol. 59, no. 12, pp. 74–80, Dec. 2021.

[3] H. S. Khallaf, S. Hashima, M. Rihan, E. M. Mohamed, and H. M. Kasem, "Quantifying impact of pointing errors on secrecy performance of UAV-based relay-assisted FSO links," *IEEE Internet Things J.*, vol. 11, no. 2, pp. 2979–2989, Jan. 2024, doi: 10.1109/jiot.2023.3297857.

[4] X. Jiang, M. Sheng, N. Zhao, C. Xing, W. Lu, and X. Wang, "Green UAV communications for 6G: A survey," *Chin. J. Aeronaut.*, vol. 35, no. 9, pp. 19–34, Sep. 2022.
[5] E. M. Mohamed, S. Hashima, and K. Hatano, "Energy aware multiarmed bandit for millimeter wave-based UAV mounted RIS networks," *IEEE Wireless Commun. Lett.*, vol. 11, no. 6, pp. 1293–1297, Jun. 2022, doi: 10.1109/LWC.2022.3164939.
[6] E. M. Mohamed, S. Hashima, A. Aldosary, K. Hatano, and M. A. Abdelghany, "Gateway selection in millimeter wave UAV wireless networks using multi-player multi-armed bandit," *Sensors*, vol. 20, no. 14, p. 3947, Jul. 2020, doi: 10.3390/s20143947.
[7] A. Amrallah, E. M. Mohamed, G. K. Tran, and K. Sakaguchi, "UAV trajectory optimization in a post-disaster area using dual energy-aware bandits," *Sensors*, vol. 23, no. 3, p. 1402, Jan. 2023, doi: 10.3390/s23031402.
[8] E. M. Mohamed, "Deployment of mmWave multi-UAV mounted RISs using budget constraint Thompson sampling with collision avoidance," *ICT Exp.*, vol. 10, no. 2, pp. 277–284, Apr. 2024, doi: 10.1016/j.icte.2023.07.011.
[9] W. T. Tutte, *Graph Theory*, vol. 21. Cambridge, U.K.: Cambridge Univ. Press, 2001.
[10] P. T. Boggs and J. W. Tolle, "Sequential quadratic programming," *Acta Numerica*, vol. 4, pp. 1–51, Jan. 1995.
[11] M. A. Khan, N. Kumar, S. A. H. Mohsan, W. U. Khan, M. M. Nasralla, M. H. Alsharif, J. Zywiolek, and I. Ullah, "Swarm of UAVs for network management in 6G: A technical review," *IEEE Trans. Netw. Service Manag.*, vol. 20, no. 1, pp. 741–761, Mar. 2023.
[12] X. Liu, Y. Liu, Y. Chen, and L. Hanzo, "Trajectory design and power control for multi-UAV assisted wireless networks: A machine learning approach," *IEEE Trans. Veh. Technol.*, vol. 68, no. 8, pp. 7957–7969, Aug. 2019.
[13] Y. Chen and W. S. Wong, "Power control for non-Gaussian interference," *IEEE Trans. Wireless Commun.*, vol. 10, no. 8, pp. 2660–2669, Aug. 2011.
[14] M. Alnakhli, S. Anand, and R. Chandramouli, "Joint spectrum and energy efficiency in device to device communication enabled wireless networks," *IEEE Trans. Cognit. Commun. Netw.*, vol. 3, no. 2, pp. 217–225, Jun. 2017.
[15] C. Yan, L. Fu, J. Zhang, and J. Wang, "A comprehensive survey on UAV communication channel modeling," *IEEE Access*, vol. 7, pp. 107769–107792, 2019.
[16] A. A. Khuwaja, Y. Chen, N. Zhao, M.-S. Alouini, and P. Dobbins, "A survey of channel modeling for UAV communications," *IEEE Commun. Surveys Tuts.*, vol. 20, no. 4, pp. 2804–2821, 4th Quart., 2018.
[17] X. Fu, T. Ding, R. Peng, C. Liu, and M. Cheriet, "Joint UAV channel modeling and power control for 5G IoT networks," *EURASIP J. Wireless Commun. Netw.*, vol. 2021, no. 1, p. 106, Dec. 2021.
[18] X. Wang, Z. Fei, J. Huang, J. A. Zhang, and J. Yuan, "Joint resource allocation and power control for radar interference mitigation in multi-UAV networks," *Sci. China Inf. Sci.*, vol. 64, no. 8, Aug. 2021, Art. no. 182307.
[19] S. Lee, S. Lim, S. H. Chae, B. C. Jung, C. Y. Park, and H. Lee, "Optimal frequency reuse and power control in multi-UAV wireless networks: Hierarchical multi-agent reinforcement learning perspective," *IEEE Access*, vol. 10, pp. 39555–39565, 2022.
[20] J. Li, S. Li, and C. Xue, "Resource optimization for multi-unmanned aerial vehicle formation communication based on an improved deep Q-network," *Sensors*, vol. 23, no. 5, p. 2667, Feb. 2023.
[21] X. Su, S. Chan, and J. H. Manton, "Bandwidth allocation in wireless ad hoc networks: Challenges and prospects," *IEEE Commun. Mag.*, vol. 48, no. 1, pp. 80–85, Jan. 2010.
[22] F. Harary, *Graph Theory*. Reading, MA, USA: Addison-Wesley, 1969.
[23] J. Zheng, J. Zhang, and B. Ai, "UAV communications with WPT-aided cell-free massive MIMO systems," *IEEE J. Sel. Areas Commun.*, vol. 39, no. 10, pp. 3114–3128, Oct. 2021, doi: 10.1109/JSAC.2021.3088632.
[24] J. Zheng, J. Zhang, H. Du, D. Niyato, B. Ai, M. Debbah, and K. B. Letaief, "Mobile cell-free massive MIMO: Challenges, solutions, and future directions," *IEEE Wireless Commun.*, early access, Feb. 5, 2024, doi: 10.1109/MWC.004.2300043.
[25] G. Poole and T. Boullion, "A survey on M-matrices," *SIAM Rev.*, vol. 16, no. 4, pp. 419–427, 1974.
[26] S. Chen, "Inequal. For M-matrices and inverse M-matrices," *Linear Algebra Appl.*, vol. 426, nos. 2–3, pp. 610–618, 2007.
[27] Q. Zhang, H. Wang, Z. Feng, and Z. Han, "Many-to-many matching-theory-based dynamic bandwidth allocation for UAVs," *IEEE Internet Things J.*, vol. 8, no. 12, pp. 9995–10009, Jun. 2021.
[28] E. M. Mohamed, K. Sakaguchi, and S. Sampei, "Wi-Fi coordinated WiGig concurrent transmissions in random access scenarios," *IEEE Trans. Veh. Technol.*, vol. 66, no. 11, pp. 10357–10371, Nov. 2017.
[29] S. Anand, S. Sengupta, and R. Chandramouli, "MAximum SPECTrum packing: A distributed opportunistic channel acquisition mechanism in dynamic spectrum access networks," *IET Commun.*, vol. 6, no. 8, pp. 872–882, 2012, doi: 10.1049/iet-com.2010.0607.

MOHAMMAD AHMED ALNAKHLI (Member, IEEE) received the B.Sc. degree in electrical engineering from Umm Al-Qura University, Mecca, Saudi Arabia, in 2008, the M.Sc. degree in electronic communication and computer engineering from the Electrical and Computer Engineering Department, University of Nottingham, Nottingham, U.K., in 2011, and the M.Sc. degree in network and security and the Ph.D. degree in electrical and computer engineering from the Stevens Institute of Technology, Hoboken, NJ, USA, in 2017 and 2019, respectively. He is currently an Assistant Professor with the Department of Electrical Engineering, Prince Sattam bin Abdulaziz University, Saudi Arabia. His current research interests include spectrum management and energy consumption in next-generation wireless networks, radio resource allocation in unmanned aerial vehicles (UAVs) and low earth orbit (LEO) satellites, the Internet of Things, energy and spectrum efficient wireless networks, 5G, 5GB and 6G systems, and cognitive radio networks.

EHAB MAHMOUD MOHAMED (Member, IEEE) received the Ph.D. degree in information science and electrical engineering from Kyushu University, Japan, in 2012. He is currently a Full Professor with the Department of Electrical Engineering, College of Engineering in Wadi Addwasir, Prince Sattam bin Abdulaziz University, Saudi Arabia. He also holds the same position with the Department of Electrical Engineering, Aswan University, Egypt. He was a Specially Appointed Researcher with Osaka University, Japan, from 2013 to 2016. He has more than 150 journals and conference papers. His current research interests include 5G/6G networks, cognitive radio networks, millimeter wave transmissions, Li-Fi technology, MIMO systems, and reconfigurable intelligent surfaces. He is a technical committee member of many international conferences and a reviewer of many international conferences, journals, and transactions, especially highly ranked IEEE TRANSACTIONS/journals. He was the General Chair of the IEEE ITEMS'16 and IEEE ISWC'18 and a guest editor in many highly ranked transactions/journals.

MOSTAFA M. FOUDA (Senior Member, IEEE) received the B.S. degree (as the Valedictorian) and the M.S. degree in electrical engineering from Benha University, Egypt, in 2002 and 2007, respectively, and the Ph.D. degree in information sciences from Tohoku University, Japan, in 2011. He is currently an Associate Professor with the Department of Electrical and Computer Engineering, Idaho State University, ID, USA. He also holds the position of a Full Professor with Benha University. He was an Assistant Professor with Tohoku University and a Postdoctoral Research Associate with Tennessee Technological University, TN, USA. He has (co)authored more than 220 technical publications. His current research interests include cybersecurity, communication networks, signal processing, wireless mobile communications, smart healthcare, smart grids, AI, and the IoT. He has guest-edited a number of special issues covering various emerging topics in communications, networking, and health analytics. He currently serves on the editorial board for the IEEE INTERNET OF THINGS JOURNAL (IoT-J), IEEE TRANSACTIONS ON VEHICULAR TECHNOLOGY (TVT), and IEEE ACCESS. He has received several research grants, including NSF Japan–U.S. Network Opportunity 3 (JUNO3).